



University of Kentucky
UKnowledge

Molecular and Cellular Biochemistry Faculty
Publications

Molecular and Cellular Biochemistry

2-17-2017

Hendra Virus Fusion Protein Transmembrane Domain Contributes to Pre-Fusion Protein Stability

Stacy Webb

University of Kentucky, stacy.webb@uky.edu

Tamas Nagy

University of Kentucky

Hunter Moseley

University of Kentucky, hunter.moseley@uky.edu

Michael G. Fried


University of Kentucky, michael.fried@uky.edu

Rebecca Ellis Dutch

University of Kentucky, rebecca.dutch@uky.edu

Right click to open a feedback form in a new tab to let us know how this document benefits you.

Follow this and additional works at: https://uknowledge.uky.edu/biochem_facpub

 Part of the [Amino Acids, Peptides, and Proteins Commons](#), [Biochemistry, Biophysics, and Structural Biology Commons](#), and the [Viruses Commons](#)

Repository Citation

Webb, Stacy; Nagy, Tamas; Moseley, Hunter; Fried, Michael G.; and Dutch, Rebecca Ellis, "Hendra Virus Fusion Protein Transmembrane Domain Contributes to Pre-Fusion Protein Stability" (2017). *Molecular and Cellular Biochemistry Faculty Publications*. 130.

https://uknowledge.uky.edu/biochem_facpub/130

This Article is brought to you for free and open access by the Molecular and Cellular Biochemistry at UKnowledge. It has been accepted for inclusion in Molecular and Cellular Biochemistry Faculty Publications by an authorized administrator of UKnowledge. For more information, please contact UKnowledge@lsv.uky.edu.

Hendra Virus Fusion Protein Transmembrane Domain Contributes to Pre-Fusion Protein Stability

Notes/Citation Information

Published in *The Journal of Biological Chemistry*, v. 292, no. 14, p. 5685-5694.

This research was originally published in *The Journal of Biological Chemistry*. Stacy Webb, Tamas Nagy, Hunter Moseley, Michael Fried, and Rebecca Dutch. Hendra Virus Fusion Protein Transmembrane Domain Contributes to Pre-Fusion Protein Stability. *J. Biol. Chem.* 2017; 292:5685-5694. © 2017 by The American Society for Biochemistry and Molecular Biology, Inc.

The copyright holder has granted the permission for posting the article here.

Digital Object Identifier (DOI)

<https://doi.org/10.1074/jbc.M117.777235>

Hendra virus fusion protein transmembrane domain contributes to pre-fusion protein stability

Received for publication, January 17, 2017, and in revised form, February 15, 2017. Published, JBC Papers in Press, February 17, 2017, DOI 10.1074/jbc.M117.777235

Stacy Webb, Tamas Nagy, Hunter Moseley, Michael Fried, and Rebecca Dutch¹

From the Department of Molecular and Cellular Biochemistry, University of Kentucky, Lexington, Kentucky 40536

Edited by Charles E. Samuel

Enveloped viruses utilize fusion (F) proteins studding the surface of the virus to facilitate membrane fusion with a target cell membrane. Fusion of the viral envelope with a cellular membrane is required for release of viral genomic material, so the virus can ultimately reproduce and spread. To drive fusion, the F protein undergoes an irreversible conformational change, transitioning from a metastable pre-fusion conformation to a more thermodynamically stable post-fusion structure. Understanding the elements that control stability of the pre-fusion state and triggering to the post-fusion conformation is important for understanding F protein function. Mutations in F protein transmembrane (TM) domains implicated the TM domain in the fusion process, but the structural and molecular details in fusion remain unclear. Previously, analytical ultracentrifugation was utilized to demonstrate that isolated TM domains of Hendra virus F protein associate in a monomer-trimer equilibrium (Smith, E. C., Smith, S. E., Carter, J. R., Webb, S. R., Gibson, K. M., Hellman, L. M., Fried, M. G., and Dutch, R. E. (2013) *J. Biol. Chem.* 288, 35726–35735). To determine factors driving this association, 140 paramyxovirus F protein TM domain sequences were analyzed. A heptad repeat of β -branched residues was found, and analysis of the Hendra virus F TM domain revealed a heptad repeat leucine-isoleucine zipper motif (LIZ). Replacement of the LIZ with alanine resulted in dramatically reduced TM-TM association. Mutation of the LIZ in the whole protein resulted in decreased protein stability, including pre-fusion conformation stability. Together, our data suggest that the heptad repeat LIZ contributed to TM-TM association and is important for F protein function and pre-fusion stability.

Enveloped viruses, including members of the paramyxovirus family, such as measles virus, mumps virus, Sendai virus, and the zoonotic Hendra virus (HeV),² utilize surface membrane

This work was supported by National Institutes of Health Grants R01 AI051517, F31AI120653, and P30GM110787. The authors declare that they have no conflicts of interest with the contents of this article. The content is solely the responsibility of the authors and does not necessarily represent the official views of the National Institutes of Health.

This article contains supplemental Tables S1 and S2 and Figs. S1 and S2.

¹ To whom correspondence should be addressed: Dept. of Molecular and Cellular Biochemistry, University of Kentucky College of Medicine, Biomedical Biological Sciences Research Bldg., 741 S. Limestone, Lexington, KY 40536-0509. Tel.: 859-323-1795; Fax: 859-323-1037; E-mail: rdutc2@uky.edu.

² The abbreviations used are: HeV, Hendra virus; F, fusion protein; TM, transmembrane domain; LIZ, leucine/isoleucine zipper; PIV5, parainfluenza virus 5; HRB, heptad repeat B; SN, staphylococcal nuclease; L/I, leucine-isoleucine; RIPA, radioimmune precipitation assay.

proteins to promote the vital steps of attachment and membrane fusion. Membrane fusion of the viral envelope and target cell membrane, a critical early step in infection, is driven by large conformational changes in surface viral fusion (F) proteins. The paramyxovirus F protein is a prototypic class I fusion protein that is initially synthesized as a homotrimer in a metastable pre-fusion conformation (1). The Hendra and Nipah virus F proteins are synthesized in the secretory pathway, trafficked to the plasma membrane, endocytosed for cleavage, and trafficked back to the cell surface in the fusogenically active conformation, $F_1 + F_2$ (2). Through this entire process, the F protein must maintain the pre-fusion conformation. Upon triggering, the F protein irreversibly folds into a post-fusion conformation, a change that includes dramatic rearrangement of the ectodomain. Stabilization of the pre-fusion conformation is critical for viral stability and function, because premature triggering would result in a fusion dead viral particle. Understanding factors that control the stability of the pre-fusion conformation therefore would provide an avenue for disrupting viral membrane fusion.

To obtain the pre-fusion structure of the paramyxovirus parainfluenza virus 5 (PIV5) F protein, a trimeric coiled coil was engineered and added to the soluble portion of the fusion protein. Without the coiled coil, the PIV5 F protein could only be crystallized in the post-fusion conformation. This suggests that the F protein requires a domain to pin the protein in its pre-fusion conformation, implicating the TM domain in pre-fusion protein stability (3). A recent study found that soluble HIV gp41 trimers, another class I fusion protein, could only be produced when the trimerization tag, foldon, was added to the protein (4). TM domains of viral F proteins have historically been characterized solely as membrane anchors. However, recent studies have shown that changes in length or single point mutations in the TM domain can result in modulation of class I, II, and III viral fusion protein expression and activity (5–10). Despite these studies, the mechanism by which these mutations alter F protein activity and function remains unclear. Although the TM domain of these proteins appears to be important, few studies have directly analyzed TM-TM interactions, which is likely a result of the difficulty of working with such hydrophobic domains. One study utilized NMR to demonstrate that the HIV gp41 TM domain forms a trimer in bicelles, further implicating the importance of TM-TM interactions (11). Additionally, TM-TM interactions have been shown to be important in several biological systems, including signaling processes mediated by receptor tyrosine kinases, so understanding factors that

HeV F protein TMD contributes to pre-fusion protein stability

affect TM-TM interactions could be implicated beyond viral membrane proteins (12–14).

A critical role for the TM domain in stability of the pre-fusion form was recently proposed for the herpes simplex virus gB (15), and several studies support the concept that viral fusion protein TM domains can self-associate, although the TM domain oligomeric form could not be determined with the assays utilized (16–18). Previously, our group utilized sedimentation equilibrium analytical ultracentrifugation to directly assess isolated TM-TM interactions. We were the first to demonstrate that paramyxovirus F protein TM domains self-associate in monomer-trimer equilibrium in the absence of the rest of the protein (19). Molecular dynamic simulations of influenza virus HA and HIV envelope glycoprotein TM domains support trimeric interactions, suggesting that stabilizing trimeric TM domain interactions may be characteristic of many viral fusion proteins (16, 20). Here, we analyzed the sequences of 140 TM domains from 19 paramyxovirus species and identified the presence of a β -branched residue heptad repeat. To understand what drives TM interactions in the Hendra virus F protein, the TM domain sequence was analyzed for association motifs; a heptad repeat leucine-isoleucine zipper (LIZ) was found in-frame with the upstream leucine zipper in the heptad repeat B (HRB) domain. Studies have previously shown that a LIZ motif can promote protein oligomerization in soluble proteins and more recently in hydrophobic environments (21, 22). Mutagenesis indicated that the HeV F LIZ is important for TM-TM interactions, as well as overall protein expression and stability. More specifically, mutation of the F protein LIZ motif resulted in reduced stability of the pre-fusion conformation of HeV F, suggesting that TM-TM interactions are important contributors to pre-fusion F protein stability. Together, our results suggest that disruption of HeV F TM-TM interactions affects the pre-fusion conformation of F and contributes to the F protein triggering process that is required to drive membrane fusion.

Results

Identification and oligomeric analysis of a L/I zipper in the HeV F TM domain

To further define elements that drive TM-TM interactions in Hendra F, we analyzed the TM domain sequence for motifs involved in protein-protein association and identified a heptad repeat leucine-isoleucine zipper that continued through the TM domain in-frame with the leucine zipper of the upstream HRB domain (Fig. 1A). Previous studies have demonstrated that L/I zippers can mediate protein-protein interactions in soluble proteins via hydrophobic collapse (21, 23–25). This motif was also found to contribute to protein interactions in a membrane environment via a knob in hole packing mechanism (22, 26). To determine whether this motif could be involved in TM-TM association in other viruses, the sequences of 140 paramyxovirus F proteins were analyzed for amino acid frequency in the predicted TM domain (supplemental Fig. S2). This analysis was composed of 19 unique viruses with multiple strains of each, representing each paramyxovirus genus except *Respirovirus* (supplemental Table S1). The predicted TM

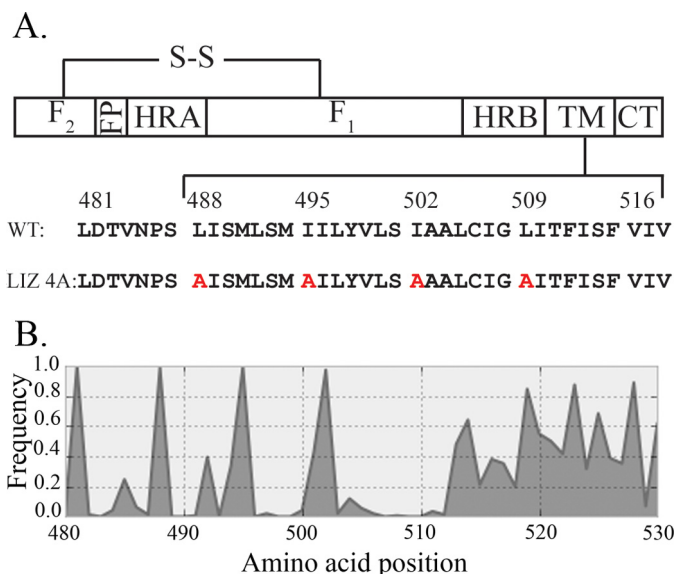


Figure 1. Schematic of paramyxovirus F protein. A, diagram of the fusogenically active, disulfide-linked heterodimer F protein with the HeV F TM sequence below. Domain structure of F includes the fusion peptide (FP), heptad repeat A (HRA), HRB, TM, and the cytoplasmic tail (CT). Mutations for the LIZ 4A HeV F construct are indicated in red in the sequence below WT F. B, the frequency of β -branched residues in the predicted TM domains of 140 viruses in the paramyxovirus family is shown graphically and appears in a heptad repeat pattern (positions 480–510).

domains were aligned to look for a specific pattern related to a leucine-isoleucine zipper. Upon examination, a heptad repeat of β -branched residues (isoleucine, valine, and threonine), which also included leucine, was identified (Fig. 1B and supplemental Table S2). This suggests that a heptad repeat, such as a L/I zipper, may be important for the TM domain across the viral family. To determine whether the predicted L/I zipper in the Hendra F TM domain contributed to TM-TM association, site-directed mutagenesis was used to replace the four L/I residues (Leu-488 + Ile-495 + Ile-502 + Leu-509) with alanine resulting in a four point mutant, LIZ 4A. To directly analyze TM-TM interactions, we utilized chimeric proteins containing staphylococcal nuclease (SN) protein linked to the TM domain of interest and analytical ultracentrifugation, as previously described (19). Samples of the wild-type SN-TM and LIZ 4A SN-TM were brought to sedimentation equilibrium in a Beckman XL-A analytical ultracentrifuge, and the radial absorbance data were obtained at 20,000, 25,000, and 30,000 rpm. The data were subjected to non-linear least squares fitting with equations modeling monomer and monomer-trimer sedimentation equilibria, as well as residual plotting with Kaleidagraph. Consistent with previous results, the data for the chimeric WT protein fit with a monomer-trimer equilibrium (Fig. 2A, blue), as determined by residual plotting (7, 19). Additional curve fits were analyzed, such as a single species monomer (Fig. 2A, red line) but were a poor fit to the absorbance points. The chimeric LIZ 4A protein also demonstrated a best fit to a shallow monomer-trimer equilibrium curve (Fig. 2B). When fit to a multispecies system (monomer-Nmer), the oligomeric state of the second species for both WT and LIZ 4A was found to be trimeric. The data points for LIZ 4A exhibited a shift in absorbance toward a smaller radial position, suggesting a shift in

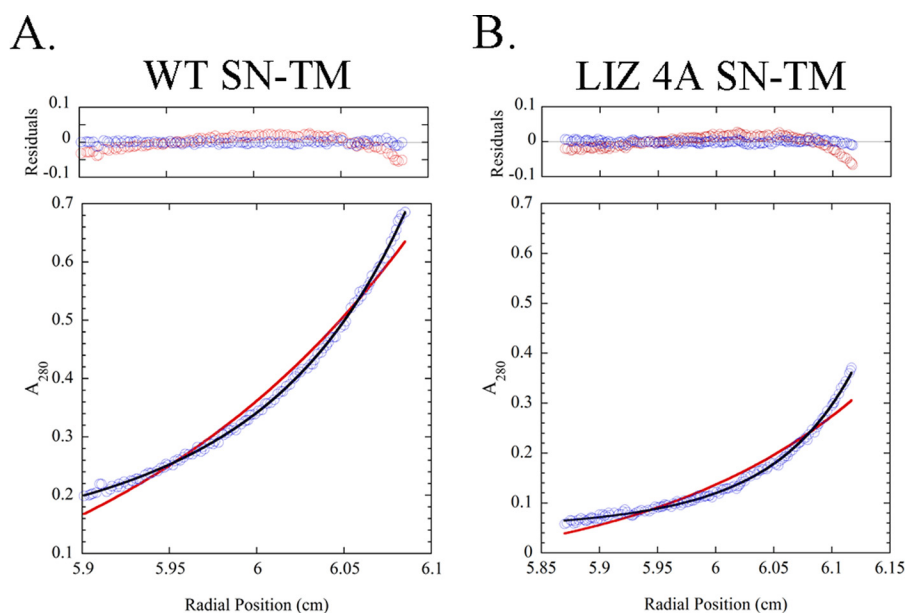


Figure 2. Sedimentation equilibrium analysis revealed a shift in monomer-trimer equilibrium for LIZ 4A SN-TM. Samples were prepared in C14SB detergent micelles, and the absorbance data were collected at 20,000 rpm in a Beckman XL-A analytical ultracentrifuge. WT SN-TM (A) and LIZ 4A (B) data points fit to a monomer (red line) and monomer-trimer (blue line) model. Residual fitting is shown above for both curve fits, with monomer residuals in red and monomer-trimer residuals in blue.

equilibrium toward a much larger population of monomeric protein when compared with WT. To further confirm this shift in equilibrium for the LIZ 4A chimeric protein, an absorbance-based apparent dissociation constant was calculated for WT and LIZ 4A. When normalized to WT at each spin speed, the LIZ 4A mutant displayed an approximately 1000-fold decrease in association constant, suggesting weaker TM-TM interactions (Table 1). These results implicate the predicted L/I zipper motif in TM-TM association for the HeV F TM domain.

Mutation of the TM domain L/I zipper alters overall protein expression and fusion activity

The analytical ultracentrifugation data suggested a shift in equilibrium upon mutation of the L/I zipper motif in the isolated TM domain, consistent with reduction in TM-TM association. To determine how these mutations affected expression, intracellular transport, and function, the LIZ 4A mutant protein was analyzed for total and surface expression by cell surface biotinylation. The trafficking and cleavage pathway of the F protein ultimately results in a homotrimer that is composed of the F_1 and F_2 fragments. The F_2 fragment is small in size, so F_1 is used to detect the cleaved, active form of F. When compared with the WT F protein, the LIZ 4A F protein exhibited a dramatic reduction in total protein expression, as indicated by the reduction in F_1 detectable (Fig. 3A). A reduction in protein expression of LIZ 4A F at the cell surface was also observed (Fig. 3B), which could potentially affect membrane fusion. The presence of cleaved F protein on the cell surface was used as a measure of whether the F protein was properly trafficked. To test fusion activity, a syncytia assay was performed in which F and the attachment protein (G) were transiently transfected into cells, and the cells were visualized for the presence of syncytia (indicated by *white arrows* in Fig. 4). The LIZ 4A F protein exhibited a striking reduction in fusion index, a measure used to

quantify fusion activity, with levels comparable with the mock control (Fig. 4). The complete loss of fusion activity exhibited by the LIZ 4A F protein indicated that the L/I zipper may contribute to overall protein stability or alter pre-fusion conformation stability. In addition, the single point mutants L488A, I495A, I502A, and L509A were examined to determine the effect each had on the F protein. The single point mutants L488A, I495A, and I502A exhibited a moderate reduction in total protein expression compared with the WT F protein (Fig. 3A). To determine the effect these mutations had on membrane fusion, syncytia formation assays were performed. Each of the single point mutants displayed a moderate to WT level fusion index (Fig. 4, A and B). The single point mutant L509A presented with a large reduction in total and cell surface protein expression levels, similar to that of LIZ 4A (Fig. 3B). Interestingly, although LIZ 4A F and L509A F had comparable reduction in total and surface expression, LIZ 4A exhibited a fusion index at background levels, whereas the L509A fusion index was only moderately reduced (Fig. 4B). Although there was a reduction in expression levels, L509A had more fusogenically active F than the LIZ 4A mutant, which would enable L509A to drive fusion, unlike LIZ 4A (Fig. 3D). A small shift in molecular weight for the LIZ 4A and L509A constructs was observed. This may be the result of altered glycosylation, because it has been shown previously that there is a glycosylation site at residue Asn-464. The change in TM-TM interactions may affect the glycosylation state or glycosylation modification of this upstream residue (28). Previously, it was shown that there is a correlation between cell surface expression and fusogenicity (29). The surface expression of LIZ 4A was ~50% of WT; however, the level of fusion activity was reduced to near background levels. This deviation suggested that LIZ 4A may be affecting overall protein stability. These results suggest that even when

HeV F protein TMD contributes to pre-fusion protein stability

Table 1

Best fit model and relative apparent association constant (K_a) for purified SN-TM constructs

Analysis was performed at three different speeds. The data are shown for monomer and monomer-trimer curve fits. Based on χ^2 and residual fitting, the monomer-trimer curve fit was most appropriate for WT and LIZ 4A. The relative apparent association constant (K_a) is normalized to the WT SN-TM construct for each spin.

		20,000 rpm		25,000 rpm		30,000 rpm	
		WT	LIZ 4A	WT	LIZ 4A	WT	LIZ 4A
Monomer fit	χ^2	0.0424	0.0485	0.2184	0.0971	0.0504	0.0221
	R	0.990	0.972	0.982	0.972	0.993	0.981
Monomer-trimer fit	χ^2	0.00184	0.00236	0.00305	0.00180	0.00303	0.00174
	R	1.000	0.999	1.000	0.999	1.000	0.999
	K_a	1	2.39×10^{-3}	1	8.37×10^{-2}	1	4.11×10^{-2}

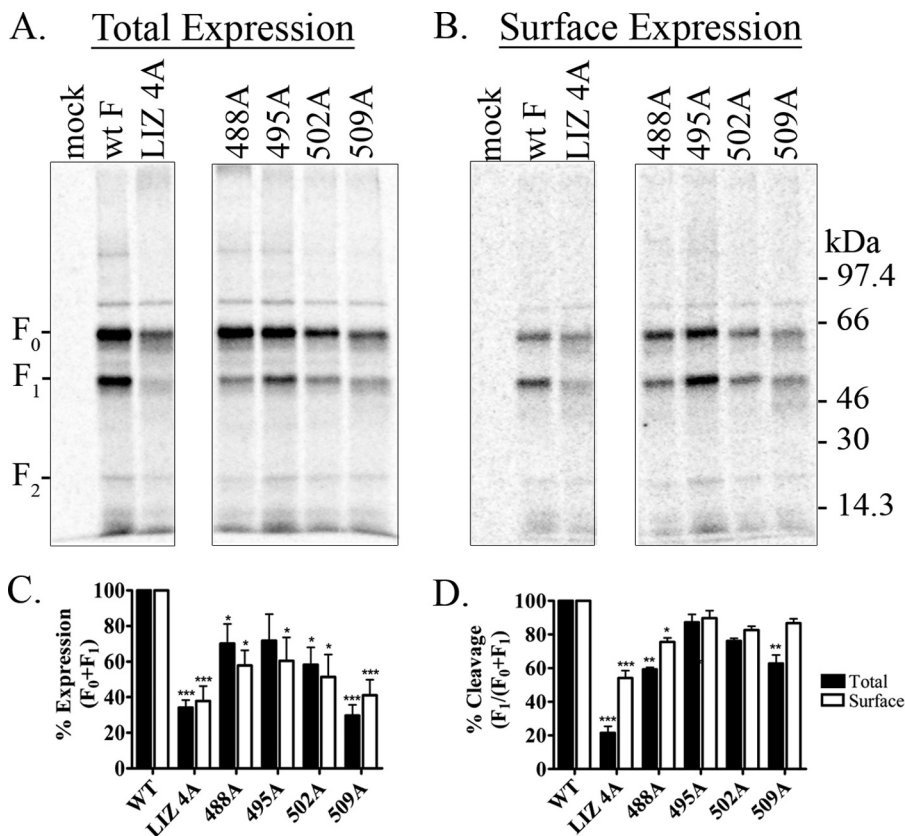


Figure 3. Total and surface expression levels for LIZ 4A F were reduced. A and B, total protein (A) and cell surface (B) expression levels of transiently transfected F constructs after a 3-h metabolic label, surface biotinylation, and immunoprecipitation. C, total (black bars) and surface (white bars) expression levels of $F_0 + F_1$ were determined by densitometry and normalized to WT levels. D, the amount of cleaved F was determined by densitometry as $F_1/(F_0 + F_1)$. The average represents three independent experiments. Each mutant was compared with the WT F protein using the Student's *t* test. *, $p < 0.05$; **, $p < 0.005$; ***, $p < 0.0005$.

individual mutations have an impact on protein expression, it was the mutation of the four L/I zipper residues that caused a complete loss of F protein fusogenic activity.

Mutation of the TM domain L/I zipper affects stability of the full-length F protein

The HeV F protein is trafficked through the secretory pathway and must then undergo a unique trafficking pathway through recycling endosomes for processing to the fusogenically active form of F by cathepsin L (2). The F protein is synthesized in the endoplasmic reticulum as an inactive trimer (F_0), trafficked to the plasma membrane, endocytosed, and cleaved to the fusogenically active form of F ($F_1 + F_2$). After cleavage, the active form of F must then be trafficked back to the plasma membrane (30). With this complicated trafficking pathway, the F protein must be stable over time so that it can ultimately arrive at the plasma membrane in its active, cleaved form.

To test whether the LIZ 4A TM mutation affected the stability of the F protein over time, a pulse-chase experiment was performed with various time points analyzed up to 24 h post-transfection (Fig. 5). The WT HeV F protein displayed stability over a 24-h time period. At early time points (0–1 h), the F protein was detected as the inactive uncleaved form, F_0 . Expression levels increased from the 0-h time point. This is likely because the C-tail antibody does not recognize partially synthesized protein at the 0-h time point. Between the 2- and 4-h time points, the F protein was detected in both the uncleaved and cleaved forms, suggesting proper trafficking and cleavage of the F protein. Ultimately at the final time points, only the cleaved, fusogenically active form of WT F was present (Fig. 5A). Interestingly, the initial level of LIZ 4A F protein expression at the early time points (0 and 0.5 h) were compara-

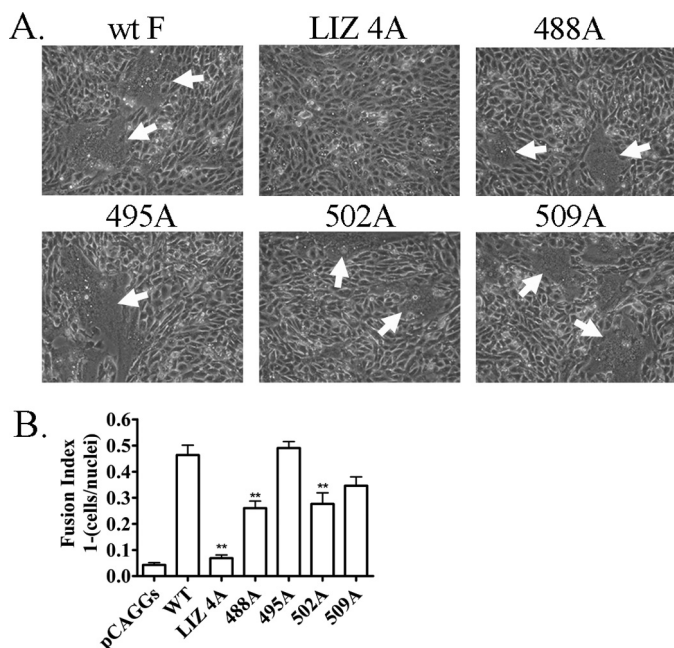


Figure 4. The LIZ 4A mutation completely abolishes F-mediated fusion activity. A, Vero cells were transfected with the HeV G attachment protein and WT F or each of the L/I zipper mutants. Syncytia formation was analyzed 24 h post-transfection; images were taken with a Nikon TS100 microscope. White arrows indicate syncytia. Images are representative. B, quantification represents three independent experiments. **, $p < 0.005$.

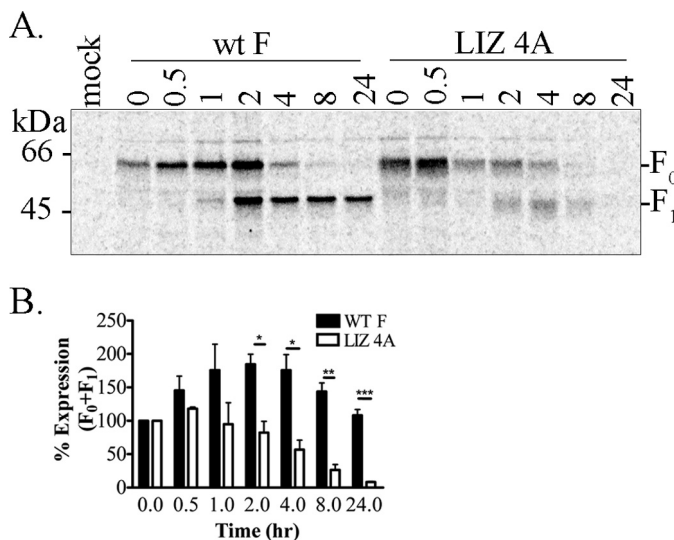


Figure 5. LIZ 4A F was less stable over time than the WT F. A, a pulse-chase experiment was performed to monitor WT F or LIZ 4A F protein expression and processing. After a 30-min metabolic label, samples were taken at various time points, immunoprecipitated, analyzed on a 15% SDS-PAGE, and exposed to a Phosphor screen for imaging. B, quantification of $F_0 + F_1$ was determined by densitometry and normalized to the 0 time point for each construct. The average represents three independent experiments \pm standard deviation. The Student's t test was used to determine significance between WT F and LIZ 4A time points. *, $p < 0.05$; **, $p < 0.005$; ***, $p < 0.0005$.

ble with that of WT, but quickly protein levels began to diminish over the later time points. The remaining LIZ 4A HeV F protein was processed as expected, but by 1 h post-transfection, a decrease in expression was evident compared with the WT F protein. At 24 h post-transfection, there was almost no detectable amount of LIZ 4A F present. Band density quantification showed the progressive loss of LIZ 4A F over time (Fig. 5B). The

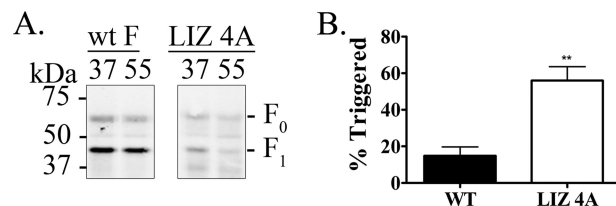


Figure 6. LIZ 4A F triggered more readily than WT F at 55 °C. A, Vero cells were transfected with WT or LIZ 4A F, thermally treated, and then antibody specific to the pre-fusion conformation of F (mAb 5B3) was directly added to cells. Immunoprecipitation was performed followed by Western blot analysis, probing for the F protein with mAb 5G7. Thermal triggering was performed at 55 °C for both constructs. B, quantification was determined via band densitometry, normalized to 37 °C for each construct, and reported as the percentage of triggered [$100 \times (1 - (F \text{ expression at } 55 \text{ °C}/F \text{ expression at } 37 \text{ °C}))$]. The results represent three independent experiments. **, $p < 0.005$.

reduction in LIZ 4A F protein did not appear to be a result of reduced protein synthesis but could be attributed to overall misfolding of the protein, resulting in targeting for degradation, or to premature triggering of F to its post-fusion conformation. It has been suggested previously that prematurely triggered F protein is more susceptible to degradation, which could explain the reduction in LIZ 4A F detection (31).

Pre-fusion F protein stability is reduced with LIZ 4A mutation

To obtain crystal structures of the pre-fusion conformation of several viral F proteins, including PIV5 F, HeV F, and respiratory syncytial virus F, trimeric tags were engineered onto the protein to prevent triggering to the post-fusion conformation (3, 4, 32, 33). This suggested that the F protein may require TM-TM association to maintain the pre-fusion conformation, until an appropriate event occurs to promote triggering to the post-fusion conformation. The LIZ 4A F protein was utilized to determine whether reduction in TM-TM association affected F protein triggering. Other groups have previously shown that changes in thermal conditions can promote triggering of the F protein (34–36). Based on the thermal triggering property of F, a novel assay was developed to test pre-fusion F protein stability. After cells were transfected to express the F protein, they were either maintained at 37 °C or exposed to an elevated temperature of 55 °C for a brief period. After heat exposure, the cells expressing the WT F protein or LIZ 4A mutant were then quickly cooled to prevent further conformational changes and incubated with an antibody, mAb 5B3, that was specific to the pre-fusion conformation of HeV F. This allowed for immunocapture of the population of F that remained in the pre-fusion conformation on the surface of the cell, thus representing the population that would drive membrane fusion. The cells were then lysed and processed to determine the amount of F protein in the pre-fusion conformation. The WT HeV F protein was only minimally susceptible to thermal triggering at 55 °C, because only ~15% of the WT protein triggered at this temperature (Fig. 6A). In contrast, the LIZ 4A F protein exhibited a dramatic reduction in pre-fusion F detectable, corresponding to ~60% of the expressed protein triggered (Fig. 6B). Additional experiments were performed with the WT HeV F protein at higher temperatures of 60 °C, at which the majority of the WT HeV F protein surface population triggered to the post-fusion conformation (supplemental Fig. S1). The susceptibility of LIZ 4A F to trigger at temperatures lower than the WT HeV F sug-

HeV F protein TMD contributes to pre-fusion protein stability

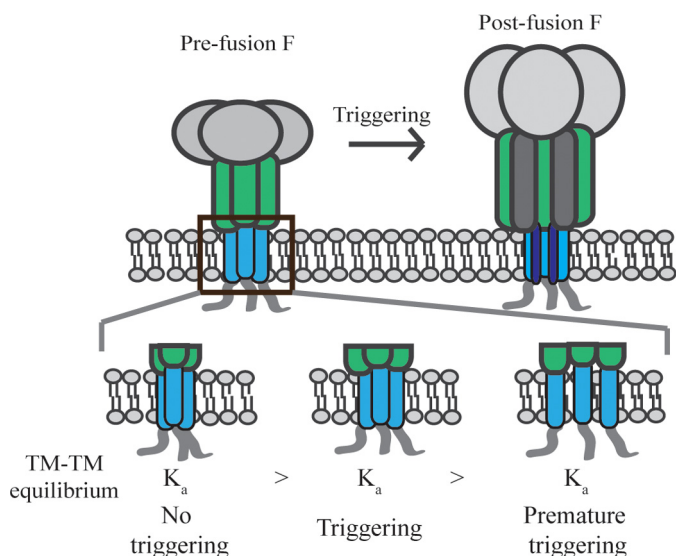


Figure 7. Proposed model: TM-TM association affects triggering. Viral fusion proteins undergo a large conformational change upon triggering. TM-TM interactions are important for maintenance of the pre-fusion conformation. Reduced TM-TM association results in prematurely triggered F protein, whereas TM-TM association that is too strong may prevent triggering to the post-fusion conformation. A dynamic equilibrium must therefore be maintained in order for the F protein to properly trigger for membrane fusion.

gested that TM-TM association may contribute to pre-fusion stability of the F protein, with a shift in TM-TM association equilibrium resulting in a dramatic effect on the stability of the pre-fusion conformation.

Discussion

Although paramyxovirus F proteins have been studied extensively, the factors driving pre-fusion stability remain unclear. Upon triggering, the F protein undergoes a dramatic conformational change, refolding to the post-fusion conformation (Fig. 7). This large, irreversible change in conformation drives membrane fusion between the viral and cellular membranes, a critical event in the viral life cycle. It has been shown that peptides that prevent conformational changes can be used as a therapeutic treatment, as in the case of enfuvirtide for targeting of HIV gp41 (37). Maintenance of the pre-fusion state of the F protein is necessary until the F protein is in the appropriate location to drive membrane fusion. Stabilization of the pre-fusion conformation is therefore critical for viral stability and function.

Although the pre-fusion structure for several viral fusion proteins has been obtained, including Nipah virus F, HeV F, HIV env, and the human coronavirus HKU1 spike protein, the structure of each required modification with a trimeric tag, such as foldon or GCNt (4, 33, 38, 39). TM domains of viral F proteins have historically been considered to act primarily as membrane anchors, but these structural studies suggest that the TM domain may be important for pre-fusion F stability, because the soluble trimeric tags mimic the proposed function of the TM domain. Previously, we have shown that several paramyxovirus F protein TM domains associate in a monomer-trimer equilibrium in the absence of the rest of the protein (19). In addition, replacement of F protein TM domains with foreign TM sequences, including a poly-leucine stretch, can result in folding defects (40–42). The TM domain of the measles virus F

protein was found to modulate fusion activity by altering F protein interaction with its receptor binding protein, hemagglutinin (10). These studies suggest that the TM domain sequence and TM-TM interactions are specific and important for the stability of the F protein. Results from the data presented here further support the importance of the TM domain in F protein function and suggest that TM-TM interactions are important for HeV F protein stability and function. More importantly, these results demonstrate the significance of TM-TM association in the stability of the pre-fusion conformation of F, a critical point of control for viral membrane fusion.

A L/I zipper was identified in the TM domain of HeV F in-frame with the upstream heptad repeat B domain. Here, sedimentation equilibrium analytical ultracentrifugation demonstrated that mutation of the L/I zipper motif resulted in reduced TM-TM association when the TM domain was studied in isolation. Previously, motifs responsible for TM-TM association in cellular transmembrane proteins include the GXXXG motif, polar amino acids, Ser/Thr clusters, and QXXS motifs. The GXXXG motif has been suggested to promote TM-TM interactions in the HIV env protein (43–45). Identification of an L/I zipper motif is a novel association motif for viral F protein TM domains (23). The sequence analysis of 140 paramyxoviruses revealed a heptad pattern of β -branched residues, suggesting that TM association motifs may be more flexible than a strictly leucine/isoleucine zipper. Mutation of the L/I zipper also resulted in alteration of overall protein stability and fusion activity, suggesting that TM-TM interactions are important for proper F protein function. The mutation of the entire L/I zipper dramatically reduced transient protein expression levels and abolished fusion activity and overall protein stability as demonstrated via pulse-chase experiments. The L/I zipper and similar motifs could also be involved in TM-TM association of other class I viral fusion proteins, but there may be multiple motifs within a single TM domain that maintain TM-TM association.

Considering the requirement of a trimerization tag for crystallization of several paramyxovirus F proteins in the pre-fusion conformation, it is reasonable to predict that TM-TM interactions are involved in maintaining pre-fusion F protein stability. Various groups have previously shown that thermal treatment can be utilized to trigger the fusion protein to its post-fusion conformation. This characteristic of the F protein was used to develop an assay that demonstrated that mutation of the L/I zipper in the HeV F TM resulted in a protein that was dramatically less stable in the pre-fusion conformation. It is important to remember that the F protein must ultimately trigger and drive membrane fusion, so equilibrium must be maintained with TM-TM interactions not being too strong or too weak. The results here suggested that shifting the TM-TM interactions toward a monomeric state dramatically destabilized the pre-fusion conformation of the F protein. The proposed model suggests that TM-TM interactions are important for stability of the F protein in its pre-fusion conformation (Fig. 7). We hypothesize that, on the other end of the spectrum, if TM-TM interactions are too strong, the F protein will not be able to trigger to the post-fusion conformation. Here we propose that TM-TM interactions could also be important *in vivo* and that modulation of those interactions may result in a fusion dead

particle as a result of premature triggering of the F protein. Together, these results suggest that TM-TM interactions serve to pin the F protein in its pre-fusion conformation, although a dynamic equilibrium ultimately allows triggering.

Beyond viral F proteins, TM-TM interactions have been shown to be important in several cellular processes. A number of studies have shown that TM-TM interactions are necessary for proper signaling of receptor tyrosine kinases, such as ErbB/Neu receptors and EGF receptor. A recent report found that targeting the ErbB TM domain with TM domain-derived peptides could delay tumor growth (13, 46). Additionally, the β -amyloid peptide, which helps mediate plaques typical of Alzheimer's disease lesions, was found to contain critical TM domain residues that contribute to β -amyloid peptide oligomerization (47). The identification of a L/I zipper in the TM domain of the Hendra viral F protein may provide insight into motifs responsible for TM-TM association in cellular proteins. These studies implicate the TM domain as not just an anchor in the membrane, but more importantly as a domain essential for the function of the full-length viral F protein. When considering methods for targeting the viral F protein for therapeutic purposes, it may be reasonable to consider targeting the TM domain, as it has been shown here to contribute to pre-fusion stability and overall F protein function.

Experimental procedures

Cell lines and culture

Vero cells (kindly provided by Robert Lamb, Howard Hughes Medical Institute/Northwestern University) were maintained in DMEM (Invitrogen) supplemented with 10% FBS.

Plasmids and antibodies

Plasmids containing Hendra F or G were generously provided by Dr. Lin-Fa Wang (Australian Animal Health Laboratory) and were subcloned into pCAGGS as described (48). The pCAGGS plasmids were transfected in Vero cells for transient expression of Hendra F or G, as described previously. All Hendra F mutants were made in pGEM using the QuikChange site-directed mutagenesis kit (Stratagene) and subcloned into the eukaryotic expression vector pCAGGS (49). SN fused to the TM domain of glycoprotein A in the pET-11a expression vector was generously provided by Karen Fleming (Johns Hopkins University) to generate the constructs described here (50). Analytical ultracentrifugation constructs containing either the wild-type or mutant Hendra F TM domain were cloned into pET11a using XmaI and XhoI sites at the 5' and 3' ends, respectively. Constructs were sequenced to confirm sequence integrity. Anti-peptide antibodies to residues 527–539 of the Hendra F cytoplasmic tail were used to pull down F. For immunoprecipitation, mAb 5G7 was used to detect the F protein in all conformations, and the pre-fusion conformation of F was detected using mAb 5B3. Both antibodies were generously provided by Dr. Christopher Broder (Uniformed Services University of the Health Sciences).

Gel electrophoresis, Coomassie staining, and Western blotting

Protein samples were analyzed via 15% SDS-PAGE, unless otherwise noted. For recombinant protein expression, protein

samples were taken pre- and post-induction to visualize protein expression via Coomassie staining. For Western blot analysis, immunoprecipitated protein was transferred to PVDF membrane (Fisher) at 50 V for 80 min. After blocking with Odyssey block buffer (Li-Cor), membranes were incubated with anti-Hendra F mouse monoclonal antibody 5G7 at a 1:3000 dilution in Tris-buffered saline with 0.05% Tween 20 (TBS-T). The membranes were washed with TBS-T and incubated with horseradish peroxidase-conjugated goat anti-mouse (light chain specific) secondary antibody (Jackson ImmunoResearch) diluted 1:10,000. The membranes were washed again with TBS-T, developed with SuperSignal West Pico Chemiluminescent substrate (Thermo Fisher), and visualized with the BioRad ChemiDoc system.

Sequence analysis

The sequences of 140 paramyxovirus F proteins were aligned and analyzed. First, the TM domains were predicted with the TMHMM Server v 2.0 (51). Next, the sequences were aligned using the MUSCLE aligner (52, 53) based on similarity that is built into the Virus Pathogen Database and Analysis Resource (VIPRBRC) (53) and cross-validated by the predicted TM domain regions. Finally, the frequency of β -branched amino acids was calculated at each position in the aligned TM domain region and graphed.

Syncytia assay

Subconfluent Vero cells in 6-well plates were transiently transfected with pCAGGS-Hendra F and pCAGGS-Hendra G at a ratio of 1:3 using Lipofectamine and Plus reagent (Invitrogen) per the manufacturer's protocol. Syncytia formation was observed 24–48 h post-transfection. The images were taken using a Nikon digital camera mounted atop a Nikon TS100 microscope with 10 \times objective. The fusion index was determined for each mutant as previously described (27). Briefly, the fusion index (f) is calculated as $f = [1 - (C/N)]$, where C is the number of cells in a field after fusion, and N is the number of nuclei.

Surface biotinylation

Vero cells (confluency 80–90%) in 60-mm dishes were transiently transfected using Lipofectamine and Plus reagent (4 μ g of DNA wild-type or mutant pCAGGS-Hendra F) according to the manufacturer's protocol. 18–24 h post-transfection, the cells were washed with PBS and starved for 45 min in DMEM deficient in cysteine and methionine. The cells were then labeled for 3 h with DMEM deficient in cysteine and methionine, containing Tran³⁵S-label (100 μ Ci/ml; MP Bio-medicals). The cells were then washed three times with 3 ml of ice-cold PBS, and surface proteins were biotinylated using 1 mg/ml EZ-Link Sulfo-NSH-Biotin (Pierce) in PBS with rocking for 35 min at 4 $^{\circ}$ C followed by incubation at room temperature for 15 min. The cells were then washed two times with ice-cold PBS, pH 8, and lysed with 500 μ l of RIPA lysis buffer (100 mM Tris-HCl, pH 7.4, 150 mM NaCl, 0.1% SDS, 1% Triton X-100, 1% deoxycholic acid, 1 mM phenylmethylsulfonyl fluoride (Sigma), and 25 mM iodoacetamide (Sigma)). Cellular lysates were centrifuged at 136,500 \times g for 15 min at 4 $^{\circ}$ C. The supernatant was

HeV F protein TMD contributes to pre-fusion protein stability

removed to a 1.5-ml microcentrifuge tube, and 4 μ l of Hendra F C-tail peptide antibody was added and incubated for 3 h at 4 °C with rocking. Proteins were then immunoprecipitated by incubating with 30 μ l of protein A-Sepharose beads (GE Healthcare) for 30 min. The beads were washed twice with RIPA + 0.30 M NaCl, twice with RIPA + 0.15 M NaCl, and once with SDS wash II (150 mM NaCl, 50 mM Tris-HCl, pH 7.4, 2.5 mM EDTA). After the beads were washed, 60 μ l of 10% SDS was added, and the samples were boiled for 10 min, removed to a new tube, and repeated with 40 μ l of 10% SDS for a total of 100 μ l. Ten microliters of the supernatant was removed to analyze the total protein population. To the remaining supernatant, 30 μ l of streptavidin beads (Pierce) and 400 μ l of biotinylation dilution buffer (20 mM Tris (pH 8), 150 mM NaCl, 5 mM EDTA, 1% Triton X-100, 0.2% bovine serum albumin) were then added for 1 h at 4 °C with rocking. Hendra F was analyzed by 15% SDS-PAGE and visualized using the Typhoon imaging system (GE Healthcare). Band densitometry using ImageQuant 5.2 was performed for each experiment to quantitate the amount of F expressed, which was reported as % expression, the sum of F_0 and F_1 , normalized to WT.

Time course immunoprecipitation

Wild-type Hendra virus F or TM mutants were transiently expressed in subconfluent Vero cells using Lipofectamine Plus (Invitrogen) as previously described. The next day cells were washed with PBS and starved for 45 min at 37 °C in cysteine-methionine-deficient DMEM. The cells were then labeled for 30 min with Trans[³⁵S] metabolic label (100 μ Ci/ml; MP Bio-medicals). At appropriate time points, the cells were washed three times with PBS and lysed with RIPA lysis buffer. Immunoprecipitation and imaging were performed as described for surface biotinylation.

Recombinant protein expression and purification

Wild-type Hendra virus F TM domain centrifugation constructs corresponding to the sequence were expressed as C-terminal fusions with staphylococcal nuclease, where the bold and underlined letters L and I below denote positions that were mutated as single point mutations, or as a four-point mutation, as indicated in Fig. 1A: VNPSLISMLSMIILYVLSIAALCIGL-ITFISFVIVEKK.

All constructs were transformed into Rosetta-Gami cells (EMD Chemicals, Gibbstown, NJ) and grown at 37 °C in 2 \times yeast extract-tryptone (YT) medium under the selection of 0.015 mg/ml kanamycin, 0.0125 mg/ml tetracycline, 0.05 mg/ml streptomycin, 0.034 mg/ml chloramphenicol, and 0.1 mg/ml ampicillin. The cultures were grown to an A_{600} of 0.6–0.8, induced for protein expression by addition of 1 mM isopropyl β -D-1-thiogalactopyranoside (Sigma), grown for 4 h, and harvested by centrifugation. The cells were resuspended in a 1:20 culture volume of lysis buffer (50 mM HEPES, 2 mM EDTA, 1 mM phenylmethylsulfonyl fluoride, pH 8.0), subjected to three freeze-thaw cycles, and incubated with 0.1 mg/ml hen egg white lysozyme for 30 min on ice. The cell lysate was then sonicated for three 20-s pulses, 5 mM CaCl₂ was added, and the solution was incubated for 30 min on ice. Insoluble protein was pelleted at 12,000 \times g for 10 min. The supernatant was then purified

using the detergent Thesit-290 (Sigma) and a single salt (1 M NH₄OAc) extraction as described previously (19), except using 50 mM HEPES instead of 20 mM Tris-HCl. The supernatant containing the recombinant protein was then dialyzed overnight at 4 °C against lysis buffer containing 0.1 M NH₄OAc and 0.2% (v/v) Thesit and clarified by centrifugation at 15,000 \times g for 15 min. The recombinant protein was purified by FPLC cation exchange chromatography using a 1-ml HiTrap SP FF column (GE Healthcare) and then exchanged into a solution containing 200 mM NaCl, 20 mM Na₂HPO₄/NaH₂PO₄ (pH 7), 29% D₂O, and Zwittergent detergent 3-(*N,N*-dimethylmyristyl-ammonio)propanesulfonate (C14SB) (Sigma), as previously described (19). Protein was dialyzed using Slide-A-Lyzer MINI dialysis units (10,000 MWCO; Pierce), and the concentrations were determined by spectrophotometry, using $\epsilon_{280} = 17,420 \text{ M}^{-1} \text{ cm}^{-1}$.

Analytical ultracentrifugation

Sedimentation equilibrium measurements were obtained at three different rotor speeds using a Beckman XL-A analytical ultracentrifuge equipped with an An-60 Ti rotor operated at 25 °C. Protein concentrations corresponding to 280-nm absorbance between 0.4 and 0.8 were utilized for determination of the best fit models. Attainment of sedimentation equilibrium was established as previously described (19). The buffer density was matched to that of C14SB detergent ($\rho = 1.04 \text{ g/ml}$) using D₂O, as described previously (19). Data analysis was performed using KaleidaGraph (Synergy Software) and HeteroAnalysis. Molecular weights for the constructs were used as constants in the analysis. The equation for curve fitting is below,

$$A(r) = \alpha_{m,0} \exp\left[\frac{M_m(1 - \bar{v}\rho)\omega^2}{2RT}(r^2 - r_0^2)\right] + \alpha_{t,0}^m \exp\left[\frac{M_m(1 - \bar{v}\rho)\omega^2}{2RT}(r^2 - r_0^2)\right] + \xi \quad (\text{Eq. 1})$$

where A represents the total absorbance of the solution at radial position (r), whereas $\alpha_{m,0}$ and $\alpha_{m,t,0}$ represent the (m) and monomer/trimer (m/t) absorbance, respectively, as the reference radius, r_0 . The molecular mass (M_m) and partial specific volume (\bar{v}) of the monomer in solution and the molecular mass for a monomer or trimer ($M_{d/t}$) as a multiple of M_m were estimated using SEDNTERP. R is the universal gas constant, T is the absolute temperature, ρ is the solvent density, ω is the angular velocity, and ξ is the baseline offset. Best fit model was chosen by examining residual distribution of approximately 0, the correlation constant (R), and χ^2 values.

Thermal triggering assay

Subconfluent Vero cells in 60-mm dishes were transiently transfected with 4 μ g of either wild-type or mutant Hendra F in pCAGGS using Lipofectamine and Plus (Invitrogen) according to the manufacturer's instructions. 18–24 h after transfection, the cells were washed and replenished with DMEM + FBS at 37 °C, or at 50 °C. Samples treated with warmed media were then incubated in a 50 °C water bath for 20 min. After heat treatment, the samples were immediately placed on ice, and the

medium was replaced with ice-cold DMEM + FBS. Following a 30-min incubation on ice, the cells were washed twice with ice-cold PBS and incubated with 5 $\mu\text{g}/\text{ml}$ mAb 5B3 in PBS + 1% BSA for 2 h at 4 $^{\circ}\text{C}$ to detect pre-fusion Hendra F. The cells were then washed twice with ice-cold PBS, lysed with RIPA + 0.15 M NaCl, and centrifuged for 15 min at $136,500 \times g$. The resultant supernatant was immunoprecipitated using protein G-Sepharose beads, and protein was analyzed via 15% SDS-PAGE. Hendra F was detected via Western blot analysis using mAb 5G7. The results were reported as follows.

$$\% \text{ triggered} = 100 \left[1 - \frac{F \text{ expression at } 55^{\circ}\text{C}}{F \text{ expression at } 37^{\circ}\text{C}} \right] \quad (\text{Eq. 2})$$

Statistical analysis

Statistical significance for the quantitative data obtained was analyzed using the Student's *t* test (*, $p < 0.05$; **, $p < 0.005$; ***, $p < 0.0005$) with GraphPad software.

Author contributions—S. W. helped develop the project, conducted most of the experiments, analyzed the results, and wrote most of the manuscript. T. N. performed the sequence analysis. H. M. provided expertise for the sequence alignment and analysis. M. F. provided expertise with the AUC experiments. R. D. developed the idea for the project and wrote the paper with SW.

Acknowledgments—We thank Dr. Karen Fleming for the kind gift of the pET11A-SN-glycophorin A construct. We thank Andreea Popa for reagent construction. We thank Dr. Christopher Broder for kindly providing monoclonal antibodies 5B3 and 5G7. We also thank the members of the Dutch laboratory for critical review of the manuscript.

Note added in proof—The first 7 amino acids in the diagram shown in Fig. 1A were incorrect in the version of this article that was published as a Paper in Press on February 17, 2017. This error has now been corrected and does not affect the results or the conclusions of the work.

References

- Harrison, S. C. (2008) Viral membrane fusion. *Nat. Struct. Mol. Biol.* **15**, 690–698
- Pager, C. T., Craft, W. W., Jr., Patch, J., and Dutch, R. E. (2006) A mature and fusogenic form of the Nipah virus fusion protein requires proteolytic processing by cathepsin L. *Virology* **346**, 251–257
- Yin, H. S., Wen, X., Paterson, R. G., Lamb, R. A., and Jardetzky, T. S. (2006) Structure of the parainfluenza virus 5 F protein in its metastable, prefusion conformation. *Nature* **439**, 38–44
- Gao, G., Wiczorek, L., Peachman, K. K., Polonis, V. R., Alving, C. R., Rao, M., and Rao, V. B. (2013) Designing a soluble near full-length HIV-1 gp41 trimer. *J. Biol. Chem.* **288**, 234–246
- Melikyan, G. B., Markosyan, R. M., Roth, M. G., and Cohen, F. S. (2000) A point mutation in the transmembrane domain of the hemagglutinin of influenza virus stabilizes a hemifusion intermediate that can transit to fusion. *Mol. Biol. Cell* **11**, 3765–3775
- Popa, A., Carter, J. R., Smith, S. E., Hellman, L., Fried, M. G., and Dutch, R. E. (2012) Residues in the Hendra virus fusion protein transmembrane domain are critical for endocytic recycling. *J. Virol.* **86**, 3014–3026
- Smith, E. C., Culler, M. R., Hellman, L. M., Fried, M. G., Creamer, T. P., and Dutch, R. E. (2012) Beyond anchoring: the expanding role of the Hendra virus fusion protein transmembrane domain in protein folding, stability, and function. *J. Virol.* **86**, 3003–3013
- Kemble, G. W., Henis, Y. I., and White, J. M. (1993) GPI- and transmembrane-anchored influenza hemagglutinin differ in structure and receptor binding activity. *J. Cell Biol.* **122**, 1253–1265
- Armstrong, R. T., Kushnir, A. S., and White, J. M. (2000) The transmembrane domain of influenza hemagglutinin exhibits a stringent length requirement to support the hemifusion to fusion transition. *J. Cell Biol.* **151**, 425–437
- Mühlebach, M. D., Leonard, V. H., and Cattaneo, R. (2008) The measles virus fusion protein transmembrane region modulates availability of an active glycoprotein complex and fusion efficiency. *J. Virol.* **82**, 11437–11445
- Dev, J., Park, D., Fu, Q., Chen, J., Ha, H. J., Ghantous, F., Herrmann, T., Chang, W., Liu, Z., Frey, G., Seaman, M. S., Chen, B., and Chou, J. J. (2016) Structural basis for membrane anchoring of HIV-1 envelope spike. *Science* **353**, 172–175
- Najumudeen, A. K., and Kajanajmudeen, A. (2010) Receptor tyrosine kinase transmembrane domain interactions: potential target for “interceptor” therapy. *Sci. Signal.* **3**, jc6
- Bublil, E. M., Cohen, T., Arnusch, C. J., Peleg, A., Pines, G., Lavi, S., Yarden, Y., and Shai, Y. (2016) Interfering with the dimerization of the ErbB receptors by transmembrane domain-derived peptides inhibits tumorigenic growth *in vitro* and *in vivo*. *Biochemistry* **55**, 5520–5530
- Aller, P., Garnier, N., and Genest, M. (2006) Transmembrane helix packing of ErbB/Neu receptor in membrane environment: a molecular dynamics study. *J. Biomol. Struct. Dyn.* **24**, 209–228
- Vitu, E., Sharma, S., Stampfer, S. D., and Heldwein, E. E. (2013) Extensive mutagenesis of the HSV-1 gB ectodomain reveals remarkable stability of its postfusion form. *J. Mol. Biol.* **425**, 2056–2071
- Kim, J. H., Hartley, T. L., Curran, A. R., and Engelman, D. M. (2009) Molecular dynamics studies of the transmembrane domain of gp41 from HIV-1. *Biochim. Biophys. Acta* **1788**, 1804–1812
- Joce, C., Wiener, A. A., and Yin, H. (2011) Multi-Tox: application of the ToxR-transcriptional reporter assay to the study of multi-pass protein transmembrane domain oligomerization. *Biochim. Biophys. Acta* **1808**, 2948–2953
- Fink, A., Sal-Man, N., Gerber, D., and Shai, Y. (2012) Transmembrane domains interactions within the membrane milieu: principles, advances and challenges. *Biochim. Biophys. Acta* **1818**, 974–983
- Smith, E. C., Smith, S. E., Carter, J. R., Webb, S. R., Gibson, K. M., Hellman, L. M., Fried, M. G., and Dutch, R. E. (2013) Trimeric transmembrane domain interactions in paramyxovirus fusion proteins: roles in protein folding, stability, and function. *J. Biol. Chem.* **288**, 35726–35735
- Victor, B. L., Baptista, A. M., and Soares, C. M. (2012) Structural determinants for the membrane insertion of the transmembrane peptide of hemagglutinin from influenza virus. *J. Chem. Inf. Model.* **52**, 3001–3012
- Harbury, P. B., Zhang, T., Kim, P. S., and Alber, T. (1993) A switch between two-, three-, and four-stranded coiled coils in GCN4 leucine zipper mutants. *Science* **262**, 1401–1407
- Gurezka, R., Laage, R., Brosig, B., and Langosch, D. (1999) A heptad motif of leucine residues found in membrane proteins can drive self-assembly of artificial transmembrane segments. *J. Biol. Chem.* **274**, 9265–9270
- Langosch, D., and Arkin, I. T. (2009) Interaction and conformational dynamics of membrane-spanning protein helices. *Protein Sci.* **18**, 1343–1358
- Harbury, P. B., Kim, P. S., and Alber, T. (1994) Crystal structure of an isoleucine-zipper trimer. *Nature* **371**, 80–83
- Ruan, W., Lindner, E., and Langosch, D. (2004) The interface of a membrane-spanning leucine zipper mapped by asparagine-scanning mutagenesis. *Protein Sci.* **13**, 555–559
- Adamian, L., and Liang, J. (2001) Helix-helix packing and interfacial pairwise interactions of residues in membrane proteins. *J. Mol. Biol.* **311**, 891–907
- White, J., Matlin, K., and Helenius, A. (1981) Cell fusion by Semliki Forest, influenza, and vesicular stomatitis viruses. *J. Cell Biol.* **89**, 674–679
- Carter, J. R., Pager, C. T., Fowler, S. D., and Dutch, R. E. (2005) Role of N-linked glycosylation of the Hendra virus fusion protein. *J. Virol.* **79**, 7922–7925

HeV F protein TMD contributes to pre-fusion protein stability

29. Smith, E. C., and Dutch, R. E. (2010) Side chain packing below the fusion peptide strongly modulates triggering of the Hendra virus F protein. *J. Virol.* **84**, 10928–10932
30. Chang, A., and Dutch, R. E. (2012) Paramyxovirus fusion and entry: multiple paths to a common end. *Viruses* **4**, 613–636
31. Farzan, S. F., Palermo, L. M., Yokoyama, C. C., Orefice, G., Fornabaio, M., Sarkar, A., Kellogg, G. E., Greengard, O., Porotto, M., and Moscona, A. (2011) Premature activation of the paramyxovirus fusion protein before target cell attachment with corruption of the viral fusion machinery. *J. Biol. Chem.* **286**, 37945–37954
32. McLellan, J. S., Chen, M., Leung, S., Graepel, K. W., Du, X., Yang, Y., Zhou, T., Baxa, U., Yasuda, E., Beaumont, T., Kumar, A., Modjarrad, K., Zheng, Z., Zhao, M., Xia, N., *et al.* (2013) Structure of RSV fusion glycoprotein trimer bound to a prefusion-specific neutralizing antibody. *Science* **340**, 1113–1117
33. Wong, J. J., Paterson, R. G., Lamb, R. A., and Jardetzky, T. S. (2016) Structure and stabilization of the Hendra virus F glycoprotein in its prefusion form. *Proc. Natl. Acad. Sci. U.S.A.* **113**, 1056–1061
34. Chan, Y. P., Lu, M., Dutta, S., Yan, L., Barr, J., Flora, M., Feng, Y. R., Xu, K., Nikolov, D. B., Wang, L. F., Skiniotis, G., and Broder, C. C. (2012) Biochemical, conformational and immunogenic analysis of soluble trimeric forms of henipavirus fusion glycoproteins. *J. Virol.* **86**, 11457–11471
35. Connolly, S. A., Leser, G. P., Yin, H. S., Jardetzky, T. S., and Lamb, R. A. (2006) Refolding of a paramyxovirus F protein from prefusion to post-fusion conformations observed by liposome binding and electron microscopy. *Proc. Natl. Acad. Sci. U.S.A.* **103**, 17903–17908
36. Paterson, R. G., Harris, T. J., and Lamb, R. A. (1984) Fusion protein of the paramyxovirus simian virus 5: nucleotide sequence of mRNA predicts a highly hydrophobic glycoprotein. *Proc. Natl. Acad. Sci. U.S.A.* **81**, 6706–6710
37. Kilby, J. M., Hopkins, S., Venetta, T. M., DiMassimo, B., Cloud, G. A., Lee, J. Y., Alldredge, L., Hunter, E., Lambert, D., Bolognesi, D., Matthews, T., Johnson, M. R., Nowak, M. A., Shaw, G. M., and Saag, M. S. (1998) Potent suppression of HIV-1 replication in humans by T-20, a peptide inhibitor of gp41-mediated virus entry. *Nat. Med.* **4**, 1302–1307
38. Xu, K., Chan, Y. P., Bradel-Tretheway, B., Akyol-Ataman, Z., Zhu, Y., Dutta, S., Yan, L., Feng, Y., Wang, L. F., Skiniotis, G., Lee, B., Zhou, Z. H., Broder, C. C., Aguilar, H. C., and Nikolov, D. B. (2015) Crystal structure of the pre-fusion Nipah virus fusion glycoprotein reveals a novel hexamer-of-trimers assembly. *PLoS Pathogens* **11**, e1005322
39. Kirchdoerfer, R. N., Cottrell, C. A., Wang, N., Pallesen, J., Yassine, H. M., Turner, H. L., Corbett, K. S., Graham, B. S., McLellan, J. S., and Ward, A. B. (2016) Pre-fusion structure of a human coronavirus spike protein. *Nature* **531**, 118–121
40. Sergel, T. A., McGinnes, L. W., and Morrison, T. G. (2000) A single amino acid change in the Newcastle disease virus fusion protein alters the requirement for HN protein in fusion. *J. Virol.* **74**, 5101–5107
41. Bissonnette, M. L., Donald, J. E., DeGrado, W. F., Jardetzky, T. S., and Lamb, R. A. (2009) Functional analysis of the transmembrane domain in paramyxovirus F protein-mediated membrane fusion. *J. Mol. Biol.* **386**, 14–36
42. Gravel, K. A., McGinnes, L. W., Reitter, J., and Morrison, T. G. (2011) The transmembrane domain sequence affects the structure and function of the Newcastle disease virus fusion protein. *J. Virol.* **85**, 3486–3497
43. Miyauchi, K., Curran, R., Matthews, E., Komano, J., Hoshino, T., Engelman, D. M., and Matsuda, Z. (2006) Mutations of conserved glycine residues within the membrane-spanning domain of human immunodeficiency virus type 1 gp41 can inhibit membrane fusion and incorporation of Env onto virions. *Jpn. J. Infect. Dis.* **59**, 77–84
44. Miyauchi, K., Curran, A. R., Long, Y., Kondo, N., Iwamoto, A., Engelman, D. M., and Matsuda, Z. (2010) The membrane-spanning domain of gp41 plays a critical role in intracellular trafficking of the HIV envelope protein. *Retrovirology* **7**, 95
45. Reuven, E. M., Dadon, Y., Viard, M., Manukovsky, N., Blumenthal, R., and Shai, Y. (2012) HIV-1 gp41 transmembrane domain interacts with the fusion peptide: implication in lipid mixing and inhibition of virus-cell fusion. *Biochemistry* **51**, 2867–2878
46. Bennisroune, A., Fickova, M., Gardin, A., Dirrig-Grosch, S., Aunis, D., Crémel, G., and Hubert, P. (2004) Transmembrane peptides as inhibitors of ErbB receptor signaling. *Mol. Biol. Cell* **15**, 3464–3474
47. Decock, M., Stanga, S., Octave, J. N., Dewachter, I., Smith, S. O., Constantinescu, S. N., and Kienlen-Campard, P. (2016) Glycines from the APP GXXXG/GXXXA transmembrane motifs promote formation of pathogenic abeta oligomers in cells. *Front. Aging Neurosci.* **8**, 107
48. Pager, C. T., Wurth, M. A., and Dutch, R. E. (2004) Subcellular localization and calcium and pH requirements for proteolytic processing of the Hendra virus fusion protein. *J. Virol.* **78**, 9154–9163
49. Niwa, H., Yamamura, K., and Miyazaki, J. (1991) Efficient selection for high-expression transfectants by a novel eukaryotic vector. *Gene* **108**, 193–199
50. Fleming, K. G., Ackerman, A. L., and Engelman, D. M. (1997) The effect of point mutations on the free energy of transmembrane alpha-helix dimerization. *J. Mol. Biol.* **272**, 266–275
51. Krogh, A., Larsson, B., von Heijne, G., and Sonnhammer, E. L. (2001) Predicting transmembrane protein topology with a hidden Markov model: application to complete genomes. *J. Mol. Biol.* **305**, 567–580
52. Edgar, R. C. (2004) MUSCLE: multiple sequence alignment with high accuracy and high throughput. *Nucleic Acids Res.* **32**, 1792–1797
53. Pickett, B. E., Sadat, E. L., Zhang, Y., Noronha, J. M., Squires, R. B., Hunt, V., Liu, M., Kumar, S., Zaremba, S., Gu, Z., Zhou, L., Larson, C. N., Dietrich, J., Klem, E. B., and Scheuermann, R. H. (2012) ViPR: an open bioinformatics database and analysis resource for virology research. *Nucleic Acids Res.* **40**, D593–D598

Hendra virus fusion protein transmembrane domain contributes to pre-fusion protein stability

Stacy Webb, Tamas Nagy, Hunter Moseley, Michael Fried and Rebecca Dutch

J. Biol. Chem. 2017, 292:5685-5694.

doi: 10.1074/jbc.M117.777235 originally published online February 17, 2017

Access the most updated version of this article at doi: [10.1074/jbc.M117.777235](https://doi.org/10.1074/jbc.M117.777235)

Alerts:

- [When this article is cited](#)
- [When a correction for this article is posted](#)

[Click here](#) to choose from all of JBC's e-mail alerts

Supplemental material:

<http://www.jbc.org/content/suppl/2017/02/17/M117.777235.DC1>

This article cites 53 references, 25 of which can be accessed free at <http://www.jbc.org/content/292/14/5685.full.html#ref-list-1>